Journal of Hydrology 432–433 (2012) 112–126

Contents lists available at SciVerse ScienceDirect

Journal of Hydrology

journal homepage: www.elsevier.com/locate/jhydrol

Aquifer denitrification and in situ mesocosms: Modeling electron donor contributions and measuring rates

Scott F. Korom [a,*], William M. Schuh [b], Tedros Tesfay [a,1], Eben J. Spencer [a]

[a] Geology & Geological Engineering, University of North Dakota, 81 Cornell Stop 8358, Grand Forks, ND 58202-8358, USA
[b] North Dakota State Water Commission, Bismarck, ND 58505-0850, USA

ARTICLE INFO

Article history:
Received 15 August 2011
Received in revised form 7 February 2012
Accepted 10 February 2012
Available online 19 February 2012
This manuscript was handled by Laurent Charlet, Editor-in-Chief, with the assistance of Bernhard Wehrli, Associate Editor

Keywords:
Aquifer denitrification
In situ mesocosms
Denitrification rates
Electron donor contributions to denitrification
Isotopic enrichment of nitrate
Nitrate contamination

SUMMARY

In situ denitrification rates were measured in a shallow unconfined glaciofluvial aquifer that had undergone large-scale nitrate contamination. Denitrification rates and isotopic enrichment factors, ε, were measured using three tracer tests in two aquifer in situ mesocosms (ISMs). Denitrification rates were also measured using a mass balance method using water samples from multiport samplers. First-order kinetic rates (k) best described the denitrification rates measured. ISM kinetic rates ranged from 0.00049/d to 0.0031/d and ε values ranged from −4.86‰ to −9.34‰; a linear relationship between k and ε values showed greater fractionation (more negative ε values) associated with higher rates. For the mass balance method, k values ranged from 0.0028/d to 0.0041/d. Combined mineralogical analysis, water quality data from the ISMs, and geochemical models using PHREEQC indicated that contributions of major electron donors to denitrification were 43–92% by organic carbon, 4–18% by pyrite, and 2–43% by non-pyritic ferrous iron, depending on the sample date and the type of amphibole used as the electron donor for ferrous iron. ISMs show promise as a tool for hydrogeochemical investigations. They are large enough to allow long-term sampling of aquifer denitrification tracer tests (>2 years), they may be used, with the modeling methodology shown herein, to estimate relative e^- donor contributions, and they limit the influence of advection and mechanical dispersion on the amended water within the chamber.

1. Introduction

Nitrate is one of the most common groundwater contaminants (Spalding and Exner, 1993; Burkart and Kolpin, 1993). Excessive nitrate in drinking water has been shown to cause methemoglobinemia in humans, particularly infants, and in livestock (McKenzie et al., 2004) and can potentially be fatal. The current US Environmental Protection Agency drinking water standard is 10 mg/L nitrate-N and that for the European Union and World Health Organization is 50 mg/L nitrate (11.3 mg/L nitrate-N).

Aquifers vary widely in their denitrifying capacities, with denitrification apparently being possible anywhere bacteria thrive and electron donors are present (Korom, 1992). Denitrification in groundwater has been identified worldwide (for example, Postma et al., 1991; Kölle et al., 1985; Mariotti et al., 1988; Phipps and Betcher, 2003; Tesoriero et al., 2000; Böhlke and Denver, 1995; Mohamed et al., 2003; Stenger et al., 2008). While most of the research cited above was conducted in shallow unconsolidated sediments, denitrification has also been reported in fractured rock aquifers. For example, Moncaster et al. (2000) and Lawrence and Foster (1986) indicated that denitrification may be occurring in fractures in chalk aquifers of the United Kingdom, wherein the primary pores are too small for bacterial colonization. Moreover, Pauwels et al. (1998) and Tarits et al. (2006) have reported denitrification occurring in fractured rock aquifers in Brittany, France.

Various electron donors have been identified in groundwater. Organic carbon has been identified as an electron donor in wetlands (Starr and Gillham, 1989) and potentially from coal fragments in aquifers (Frind et al., 1990; Postma et al., 1991). Another common electron donor is pyrite (FeS_2), which is produced by the reduction of iron and sulfate by organic matter in seabottom muds. Sulfide and ferrous iron [Fe(II)] from pyrite have been identified as primary electron donors at many locations (for example, Kölle et al., 1985; Postma et al., 1991; Korom et al., 2005; McMahon et al., 1999; Moncaster et al., 2000). A common source of pyrite is in Cretaceous shales (Golhaber and Kaplan, 1974). McMahon et al. (1999) identified the source of denitrification in the South Platte River alluvial aquifer in northeastern Colorado as pyrite in the underlying Cretaceous Pierre Formation. They found that the rate of denitrification was determined by the slow rate of nitrate transport into the shale bedrock. Increasingly investigators are reporting that denitrification in aquifers may be the result of all three major electron donors: inorganic sulfide in pyrite,

* Corresponding author. Tel.: +1 701 777 6156.
E-mail address: scott.korom@engr.und.edu (S.F. Korom).
[1] Present address: AECOM Orange Office, 999 Town and Country Road, Orange, CA 92868, USA.

0022-1694/$ - see front matter © 2012 Elsevier B.V. All rights reserved.
doi:10.1016/j.jhydrol.2012.02.023

Fe(II) from pyrite and other Fe(II)-bearing minerals, and organic carbon (for example, Böhlke and Denver, 1995; Böhlke et al., 2002; Pauwels et al., 1998, 2000).

In glaciated areas of the northern Great Plains of North America, glaciofluvial aquifers of Pleistocene or early post-Pleistocene origin are often formed from elutriated sediments consisting of glacially-produced detritus from Cretaceous shales. In eastern North Dakota and South Dakota (USA) and Manitoba (Canada) common parent materials are the high-organic shales of the Greenhorn, Carlile, Niobrara, and Pierre Formations, particularly the Pembina Member of the Pierre Formation, which is known to have relatively high pyrite contents (Tourtalot, 1962; Gill and Cobban, 1965; Hansen and Kume, 1970; Schultz et al., 1980). In some glacial aquifers overlying these formations, the sand fraction can include substantial amounts of shale fragments (10–50%). An example is the Elk Valley aquifer in Grand Forks County, northeastern ND, which has been shown to have pyrite-S as high as 1% of the grain–matrix mass (Schuh et al., 2006), and for which a zero-order denitrification rate of 0.016 mM/d (0.23 mg/L/d) was measured (Korom et al., 2005). However, farther west, such as at the Karlsruhe site described further herein, shale deposits decrease in organic matter, and bedrock parent materials consist of sands and sandstones of the Fox Hills, Belle Fourche, and Cannonball Formations. For this reason, sediments forming glaciofluvial aquifers are expected to vary widely in their denitrifying capabilities.

Because of the widespread prevalence of nitrate contamination on a worldwide scale, and because of the expense and difficulty of measuring denitrification in situ, simplified measurement methodologies and increased knowledge of potential contributions of varying electron donors would be beneficial for many remedial applications. The purpose of the project described in this paper was to determine the likely contribution of natural denitrification for remediation of an aquifer that had undergone large-scale contamination from combined point and non-point sources. The objectives, presented in this paper, were to:

(1) Compare the efficacy of three methods for quantifying denitrification rates in an aquifer, including (a) direct in situ measurements using mesocosms (Korom et al., 2005), (b) inference using the relationship found between ^{15}N fractionation and the in situ rates mentioned above, and (c) a simple stratified mass balance method;
(2) identify potential electron (e^-) donors present in the sediments;
(3) determine the kinetic rates (zero-order or first-order) for denitrification in sediments having varied and complex e^- donor sources; and
(4) estimate the contributions of e^- donors [inorganic sulfide, Fe(II), and organic C] to denitrification.

1.1. Study area description

The Karlsruhe aquifer is an unconfined coarse deposit of Wisconsinan glaciofluvial origin and underlies about 19,000 ha of agricultural land in McHenry County, north-central North Dakota (Fig. 1). It consists of sand and gravel sediments about 6–25 m thick, which were formed of outwash from a southeastward glacial advance. A likely source of the parent materials is surficial outcrops of the Cannonball Formation, which consists locally of lenticular sands, sandstones, siltstones and mudstones, and differs

Fig. 1. Location of the Karlsruhe aquifer.

considerably from the shales and high-bentonite mudstones normally found in the pyrite-rich Pierre and Carlile Formations located eastward. Part of the Karlsruhe aquifer overlies another glaciofluvial deposit, the New Rockford aquifer of an earlier southwestward ice advance, which may have derived sediments from the Cannonball Formation, or possibly another sandstone and mudstone formation known as the Fox Hills Formation. The Karlsruhe aquifer is mostly separated from the underlying New Rockford aquifer by several meters of argillaceous till, but the two are connected in the northwest portion of the Karlsruhe aquifer (Fig. 2). Recharge, from an average of 428 mm of annual precipitation, occurs primarily in the uplands to the south, and groundwater flow in the western half of the aquifer is split at an approximate central divide toward the Souris River to the west and north, and toward the Wintering River in the middle of the aquifer. Flow in the eastern portion of the aquifer is toward the Wintering River (Fig. 2). The underlying New Rockford aquifer flows northwestward toward the Souris River. Overlying soils are predominantly sandy, with some till cap located in the northwestern portion of the aquifer. Crops grown include small grains, corn, soybeans, and potatoes. During the 1990s irrigated potatoes became a major local crop and irrigated acreage increased from about 50 ha in 1974 to about 2200 ha in 2001.

Following 4 years of drought from 1988 through 1992 (for example 241 mm of precipitation fell in 1988), a period of unusually high precipitation began in North Dakota in 1993 (for example 630 mm of precipitation fell that year). The resulting increase in recharge apparently led to increased nitrate transport through the coarse vadose zone. In 1998 almost half of the 23 wells sampled by the North Dakota Department of Health in the Karlsruhe aquifer had elevated nitrate, many above the EPA drinking water limit (Bartelson and Goven, 1998). In 2001 and 2002 a monitoring well network consisting of 67 nested well sites, including 12 multiport sampler sites, was constructed in the Karlsruhe aquifer (Fig. 2). Based on vertical and horizontal integration of nitrate-N loads (Schuh et al., 2002), it was estimated that about 1.8 million kg of nitrate-N had contaminated the aquifer. In order to design an effective remediation strategy it was considered important that the denitrifying capabilities of the aquifer be understood.

2. Methods

Five complementary strategies were used to evaluate the denitrification potential of the Karlsruhe aquifer. These were:

(1) Measure e^- donor concentrations in aquifer sediment samples;
(2) measure in situ sediment denitrification rates using aquifer in situ mesocosms (ISMs);
(3) model the evolution of groundwater in situ mesocosms (ISMs) to identify the e^- donors involved and their denitrification contributions;
(4) use $\delta\,^{15}N$ and $\delta\,^{18}O$ isotope measurements for water samples collected from the ISMs and stratified samplers to evaluate the spatial extent of denitrification and the source of denitrified nitrate, and;
(5) use mass balance computations to measure denitrification rates at the stratified sample sites.

The use of ISMs provided the data necessary to provide accurate denitrification rates, to determine a linear relationship for the Karlsruhe aquifer between denitrification rates and apparent isotopic enrichment factors, and to identify the e^- donors involved in the

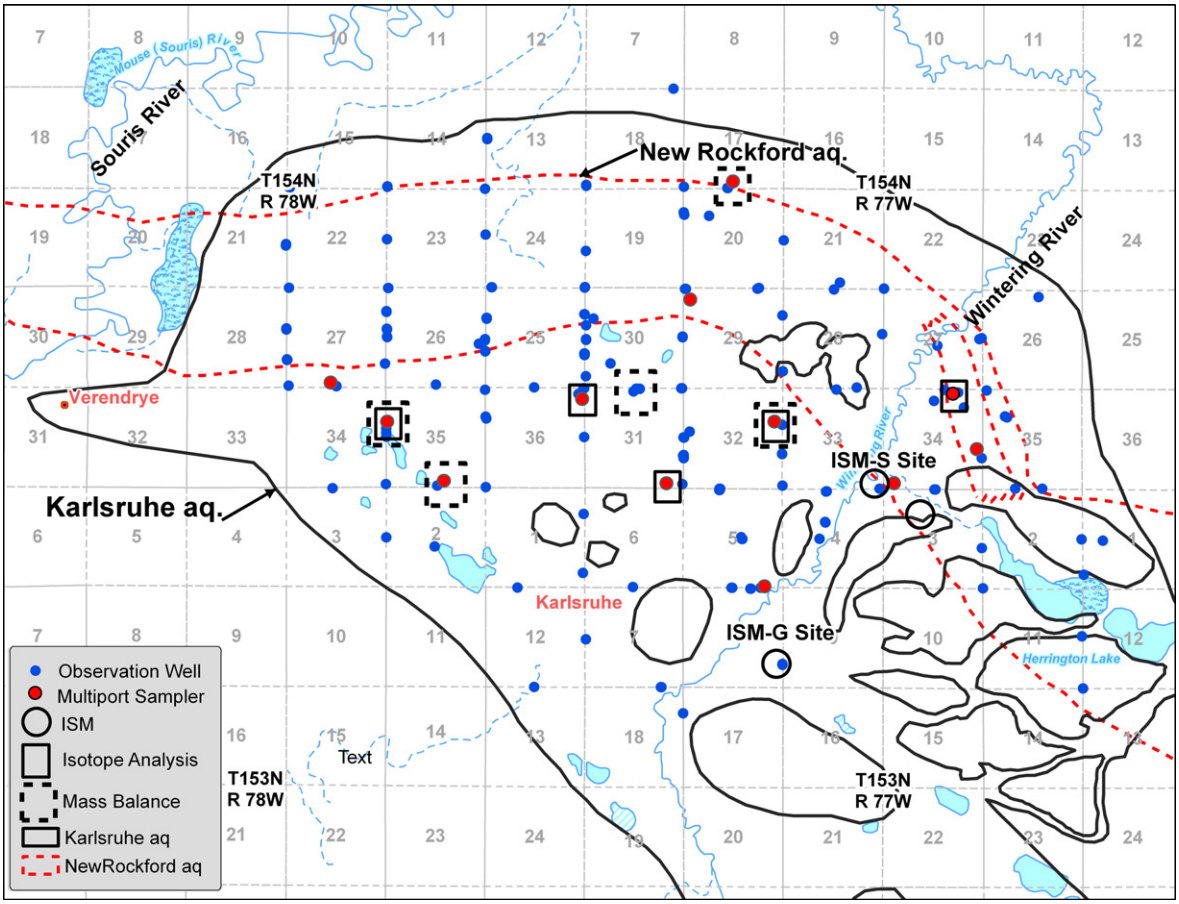

Fig. 2. The Karlsruhe aquifer with sampling sites.

Table 1
Total sulfide (S) and total organic carbon (TOC) measured for sediment samples from multiport sampler (MPS) sites in the Karlsruhe aquifer.

Site No.	Location (USBLM)	Depth Interval (m)	Sulfide-S% dry wt.	TOC% dry wt.
2	154-078-35DCC	3.7–4.3	0.01	0.02
2	154-078-35DCC	6.1–6.7	0.09	0.15
2	154-078-35DCC	8.5–9.1	0.04	0.08
9	154-077-29BBB5	4.6–5.2	<0.01	0.02
9	154-077-29BBB5	6.4–7	<0.01	0.01
9	154-077-29BBB5	8.5–9.1	0.13	0.07
10	154-077-17CDD	6.7–7.3	0.01	0.01
10	154-077-17CDD	9.1–10.1	<0.01	0.01
10	154-077-17CDD	11.3–11.9	0.11	0.02
12	154-077-34ABBA	1.5–2.1	0.02	0.01
12	154-077-34ABBA	4.6–5.2	0.05	0.05
12	154-077-34ABBA	8.8–9.5	0.06	0.32
13	154-077-32ADA	1.8–2.4	<0.01	0.02
13	154-077-32ADA	6.7–7.9	0.08	0.60
13	154-077-32ADA	8.5–9.1	0.03	0.93
16	153-077-05DDC	2.1–2.7	0.02	0.05
16	153-077-05DDC	6.7–7.3	0.18	0.59
16	153-077-05DDC	10.7–11.6	0.05	0.64
19	154-077-33DDD	1.8–2.1	<0.01	0.02
19	154-077-33DDD	6.7–7.3	0.09	0.09
19	154-077-33DDD	11.6	0.05	0.06

denitrification reactions and the amounts of denitrification they caused, the last being, as far as we know, a first in the literature. Because denitrification estimates using mass balance calculations with multiport samplers is cheaper to employ than ISMs, and allows for evaluation of a wider area of the aquifer, we also used the ISM measurements to evaluate the mass balance approach.

2.1. Aquifer sediment samples

A preliminary assessment of potential electron donors as sulfide and total organic carbon (TOC) was conducted on 21 stratified sediment samples from seven multiport sampler (MPS) sites (Table 1). Sediment samples were collected using split-spoon samplers in a hollow-core auger during construction of the MPS sites. TOC was measured using high-temperature combustion with a non-dispersive infrared gas analyzer on a Shimadzu TOC 5050 Analyzer with a Shimadzu 5000 solid sample module (Churcher and Dickhout, 1987). Pyrite, FeS_2, was the only sulfide mineral detected by XRD (Tesfay, 2006); however, amorphous iron sulfide may also be present at the site. All inorganic sulfide concentrations (crystalline and amorphous) were determined using chromium reduction (Canfield et al., 1986). Herein, for simplicity, all inorganic sulfides present at the site are referred to as "pyrite" or "FeS_2."

At the ISM sites, sediment samples were taken from 6.6 to 6.9 m at the G site and from 4.9 to 5.5 m at the S site. Particle sizes were determined using sieves and hydrometers (ASTM, 1993). TOC and inorganic sulfide contents of the sediments were determined as described above. For the S site the method of Heron et al. (1994) was used to determine amorphous Fe(II); Fe(II) minus FeS_2 was determined using chemical extraction (Kennedy et al., 1999) as adapted by Tesfay (2006); total Fe(II) was calculated by adding the Fe(II) associated with the inorganic sulfide (as FeS_2) measured in each sample. For the G site only amorphous Fe(II) was measured. Geochemical analyses were only done on sediments smaller than gravel (<2 mm). At the S site X-ray diffraction (XRD) was used to analyze sediment mineralogy and Mössbauer spectroscopy was used to help identify the iron minerals present and their fractions of Fe(II) and Fe(III).

2.2. In situ mesocosms

In situ denitrification rates in aquifer sediments were measured using stainless steel isolation chambers called "in situ mesocosms," which are driven into the aquifer formation below the redoxycline and used for controlled measurements of nitrate loss and resulting changes in water chemistry (Korom et al., 2005). Gillham et al. (1990) used a small (1.9-L) stainless steel isolation chamber called an "in situ microcosm" to conduct denitrification tracer tests, and they found that the use of isolation chambers simplified results and interpretations for denitrification experiments. Citing Gillham's work, Bates and Spalding (1998) conducted a denitrification study using larger 11-L in situ microcosms. Schlag (1999) developed a large (186-L) cylindrical stainless steel chamber 0.39-m in diameter and 1.5-m long and called it an "in situ mesocosm" (ISM); they were employed at our G and S sites. The advantage of ISMs is that they allow relatively large samples (~1 L/month) to be collected regularly for long periods (>2 years), such that the resulting chemical evolution of the groundwater within the chamber may be monitored. The ISMs were first used in the Elk Valley aquifer in northeastern North Dakota (Korom et al., 2005). So far, they have been used at six additional sites in North Dakota (including the two near Karlsruhe discussed herein), four sites in Minnesota, and two sites in Iowa.

The construction, placement and use of ISMs are described in detail in Korom et al. (2005). Avoidance of adding surface detritus, particularly organic-rich topsoil, is critical to placement. In summary, topsoil is removed and a 0.61-m diameter temporary casing is driven to the desired placement depth, usually about 2 m below the unoxidized boundary (evaluated by drilling a nearby pilot hole). Sediment is removed using a sand bailer. The ISM is then driven into the undisturbed sediments below the temporary casing; flexible tubing housed in stainless steel pipe connects the ISM to the ground surface. The temporary casing is then removed slowly and in stages to allow the natural formation to collapse around the ISM and the riser pipe. Above the water table vadose materials are then replaced in appropriate layers. Warne (2004) showed that a submersible pump can also be successfully mounted in a housing above the ISM and used for pumping from installation depths below levels where suction lift (~10 m) is feasible.

Two ISMs were placed in the Karlsruhe aquifer about 3.3 km apart: ISM-G at 153-77-8DDA (Locations identified using US Bureau of Land Management nomenclature.) and ISM-S at 154-77-33DDD (Fig. 2). ISM-G was placed 6.1–7.6 m below land surface; ISM-S was placed 4.9–6.4 m below land surface.

After installation in July 2003, the ISMs were purged of about 200 L (>3 pore volumes) to assure that natural formation water

occupied the ISMs. About 83 L of groundwater was then pumped from each ISM into a reservoir with the tubing outlet placed on the bottom of the reservoir to avoid air contact for all but the earliest drawn water. Reservoir water was amended with 50.4 g of sodium nitrate ($NaNO_3$) and 6.4 g of sodium bromide (NaBr), stirred, and then siphoned back into the ISMs; the reservoir was periodically stirred gently to keep it well-mixed during the injection period. After amendment on 7 August 2003, the ISMs were first sampled on 25 August 2003 and sampled subsequently about every 2 months. Groundwater samples were filtered (0.45 μm) and analyzed using the standard methods listed on Table 1b in Korom et al. (2005). Field measurements for pH were used except on 20 October 2003, 19 November 2003, 19 July 2004, and 22 September 2005 when lab values were recorded because of apparent problems with the field meter or because field measurements were not taken. Br in the amended water was used to determine the dilution rate with native groundwater. Loss of nitrate beyond that explained by dilution of the Br tracer was attributed to denitrification. Further evidence of denitrification was provided by the enrichment of ^{15}N in the nitrate remaining in the ISMs.

Both zero- and first-order denitrification rates were calculated for the ISM tracer tests. The former were calculated by plotting the amount of nitrate lost, beyond that explained by dilution of the Br tracer, versus time. First-order rates were determined by plotting the natural logarithm of the relative nitrate concentrations, corrected for Br dilution [Haggerty et al., 1998, Eq. (10)], versus time. Best-fit slopes, or reaction rates, for both types of data sets were found using linear regression. Nitrate was lost in ISM-S relatively quickly and the first tracer test (“ISM-S1”) was stopped on 24 May 2004 when the ISM was purged and amended a second time using the same procedure. The initial sample for the second tracer test in ISM-S (“ISM-S2”) was collected on 1 June 2004. ISM-S2 and the first and only test in ISM-G were sampled through 22 September 2005. Background Br concentrations for all tracer tests were <0.01 mM and assumed to be 0; background nitrate-N concentrations were <0.07 mM and assumed to be 0; the background Na concentration for ISM-G was 9.16 mM, for ISM-S1 it was 1.54 mM, and for ISM-S2 it was 1.13 mM.

2.3. Geochemical modeling

PHREEQC (Parkhurst and Appelo, 1999), a computer program developed by the US Geological Survey for simulating geochemical reactions, was used to model the changes in groundwater quality during the denitrification tracer tests in the ISMs to provide insights on the contributing e^- donors. Water quality data from the ISMs (Table 2) were used to calculate saturation indices [SI = log (ion activity product/equilibrium constant)] for the following minerals: barite ($BaSO_4$), gypsum ($CaSO_4{\cdot}2H_2O$), epsomite ($MgSO_4{\cdot}7H_2O$), jarosite-K [$KFe_3(SO_4)_2(OH)_6$], calcite ($CaCO_3$), magnesite ($MgCO_3$), and quartz (SiO_2). During modeling, analyte concentrations <detection were set equal to 90% of their detection limit, except for Br and nitrate-N, which were set equal to 0. Thermodynamic data for the minerals were from the “phreeqc.dat” database, except for epsomite and magnesite, which were from the “minteq.v4.dat” database.

Water samples were drawn from the top of the ISMs (Korom et al., 2005) on the dates shown on Table 2. The water column in the ISM was slowly pulled upward with each sampling event; each groundwater sample collected would have interacted with sediments under slightly different spatial and different temporal conditions. Because the sediments in the ISMs were considered to be chemically heterogeneous, chemical species for each succeeding water sample were compared to the initial sample to estimate denitrification amounts and to determine which e^- donors may have contributed to the denitrification.

The first step for characterizing the evolution of groundwater quality in the ISMs required the determination of whether denitrification had taken place in an ISM ground water sample. For each water sample after the initial one, a “Br dilution factor” was calculated by dividing its Br concentration by the initial Br concentration. If the ratio of the subsequent nitrate concentration to the initial nitrate concentration was < that predicted by the Br dilution factor, the difference was attributed to denitrification. If the subsequent nitrate concentration was ⩾ that predicted by the Br dilution factor, no denitrification was detected and no further analysis of the data for that sampling date was performed. Such observations only occurred twice and both were during the early part of the ISM-G tracer test (20 October 2003 and 23 March 2004), as noted on Table 2.

The second step was to input the appropriate water quality data into the model. The data (see Table 2) for the initial water sample were copied into PHREEQC, with only three of the analyte values changed to prepare the data for the analysis of each subsequent sample. The Br concentration was changed to the value measured in the subsequent sample, the nitrate concentration was calculated by multiplying the initial nitrate-N concentration by the Br dilution factor, and the Na concentration was calculated by using the Br dilution factor to determine the fraction of the sample that was comprised of the amended water (with NaBr added to it) and the fraction that was comprised of the native (“background”) water.

The third step involved reacting the modified initial sample analytical data from step 2 with e^- donors to determine what mix of donors best explained the evolving water quality measured in the ISMs during the subsequent sampling event. This step requires a description of the e^--donating reactions considered.

The three common e^- donors for denitrification (Korom, 1992) are organic carbon (OC), Fe(II), and pyrite [14/15 of electrons from sulfide and 1/15 from Fe(II)]. The reaction added to PHREEQC for the oxidation of organic carbon was:

$$CH_2O + H_2O \leftrightarrow CO_2 + 4H^+ + 4e^- \quad (1)$$

Modeling denitrification with Fe(II) was more complicated. XRD measurements indicated that the dominant minerals were quartz, plagioclase and alkali feldspars, calcite and dolomite, with small amounts of the following minerals, which may contain Fe(II), also present: clinochlore, biotite (or possibly muscovite), amphibole, and pyrite (Tesfay, 2006). Mössbauer results corroborated the presence of clinochlore and amphibole and indicated the fraction of Fe(II) to total Fe in the sediments ranged from 50% to 65% (Tesfay, 2006). In addition, major cation results (Na, K, Ca, and Mg) on Table 2 show the following features:

(1) Considering the background concentrations of Na and Br (given above) in the native groundwater in the ISMs, Na concentrations were reasonably approximated by dilution, as determined by the Br tracer (except for the latter half of ISM-S2, where Na concentrations apparently increased above that explained by dilution of the amended water by native groundwater). This suggests that cation exchange processes were generally insignificant at the ISM sites, a finding consistent with the coarse texture of the sediment in both ISMs. It also suggests that there were no significant inputs of Na associated with denitrification in ISM-G and for most of the testing done in ISM-S.
(2) K concentrations remained constant during the tracer tests.
(3) Ca/Mg ratios we relatively constant throughout the tests, indicating that any sources or sinks affected both cations similarly.

Table 2
Concentrations of dissolved ions measured in water samples collected from tracer tests in the Karlsruhe in situ mesocosms. All analyte values are mM, except for pH, which is in standard units, and $\delta^{15}N$, which is in permil.

Date	Days	Na	K	Ca	Mg	Mn	Fe	NH_3-N	Al	Ba
Karlsruhe ISM-G										
25 Aug 2003	0	15.1	0.26	1.51	1.82	0.008	<0.00018	<0.00071	<0.0019	0.0014
20 Oct 2003[a]	56	13.8	0.28	1.55	1.90	0.011	0.00036	<0.00071	<0.0019	0.0014
22 Dec 2003	119	13.1	0.25	1.46	1.71	0.008	0.00020	<0.00071	<0.0019	0.0013
23 Mar 2004[a]	211	13.2	0.27	1.52	1.77	0.010	0.00023	<0.00071	<0.0019	0.0015
1 Jun 2004	281	12.4	0.26	1.49	1.74	0.010	0.00025	<0.00071	<0.0019	0.0014
19 Jul 2004	329	12.1	0.25	1.47	1.73	0.010	0.00018	<0.00071	<0.0019	0.0015
13 Sep 2004	385	11.6	0.24	1.42	1.71	0.010	0.00027	<0.00071	<0.0019	0.0014
6 Dec 2004	469	11.0	0.25	1.41	1.69	0.010	<0.00018	<0.00071	<0.0019	0.0018
3 Feb 2005	528	11.4	0.26	1.46	1.72	0.011	0.00029	<0.00071	0.0027	0.0013
12 Apr 2005	596	11.4	0.26	1.48	1.75	0.011	0.00021	<0.00071	<0.0019	0.0013
14 Jun 2005	659	11.5	0.27	1.53	1.81	0.012	0.00036	<0.00071	<0.0019	0.0014
2 Aug 2005	708	10.6	0.25	1.43	1.66	0.011	0.00088	<0.00071	<0.0019	0.0013
22 Sep 2005	759	10.8	0.26	1.42	1.67	0.011	0.00054	0.00878	<0.0019	0.0013
	SiO_2	pH	F	Cl	SO_4	NO_3^-—N	Br	Inorg C	$\delta^{15}N$	
25 Aug 2003	0.361	7.39	0.0047	0.36	0.527	5.33	0.561	14.2	1.93	
20 Oct 2003[a]	0.361	7.63	0.0048	0.35	0.496	4.82	0.507	13.4		
22 Dec 2003	0.336	7.65	0.0054	0.37	0.487	4.33	0.466	14.8		
23 Mar 2004[a]	0.356	7.75	0.0055	0.37	0.497	3.29	0.338	15.4	5.36	
1 Jun 2004	0.338	7.42	0.0044	0.35	0.551	3.29	0.369	14.2		
19 Jul 2004	0.335	7.90	<0.0026	0.36	0.544	2.83	0.332	14.5		
13 Sep 2004	0.333	7.46	0.0089	0.36	0.560	2.53	0.304	13.5	4.89	
6 Dec 2004	0.333	7.17	0.0054	0.35	0.572	2.08	0.263	14.5		
3 Feb 2005	0.338	7.60	0.0045	0.34	0.549	1.72	0.222	14.7		
12 Apr 2005	0.335	7.47	0.0051	0.34	0.581	1.68	0.227	14.6	9.52	
14 Jun 2005	0.346	7.78	0.0049	0.34	0.582	1.49	0.208	14.8		
2 Aug 2005	0.326	7.75	0.0049	0.36	0.610	1.46	0.205	14.7		
22 Sep 2005	0.326	7.69	0.0051	0.35	0.564	1.14	0.171	14.7	8.87	
	Days	Na	K	Ca	Mg	Mn	Fe	NH_3-N	Al	Ba
Karlsruhe ISM-S Tracer Test 1										
25 Aug 2003	0	8.48	0.14	2.62	1.70	0.015	0.00018	0.00842	<0.0019	0.0029
20 Oct 2003	56	7.66	0.15	2.40	1.56	0.016	<0.00018	Not done	<0.0019	0.0026
19 Nov 2003	86	6.83	0.15	2.20	1.44	0.014	0.00036	0.00807	<0.0019	0.0025
22 Dec 2003	119	5.96	0.14	2.05	1.33	0.013	<0.00018	<0.00071	<0.0019	0.0020
18 Feb 2004	177	5.83	0.15	2.17	1.42	0.014	0.00023	<0.00071	<0.0019	0.0026
23 Mar 2004	211	5.48	0.15	2.12	1.39	0.014	<0.00018	0.00129	<0.0019	0.0022
24 May 2004	273	4.87	0.14	2.10	1.38	0.013	0.00030	<0.00071	<0.0019	0.0022
	SiO_2	pH	F	Cl	SO_4	NO_3^-—N	Br	Inorg C	$\delta^{15}N$	
25 Aug 2003	0.363	7.56	0.0050	0.15	1.16	6.30	0.637	7.68	0.63	
20 Oct 2003	0.296	7.58	0.0057	0.13	1.18	5.25	0.602	7.68		
19 Nov 2003	0.261	7.50	0.0063	0.14	1.27	3.63	0.482	7.63	5.09	
22 Dec 2003	0.240	7.70	0.0062	0.14	1.23	3.08	0.457	7.74		
18 Feb 2004	0.250	7.74	0.0057	0.13	1.32	2.31	0.397	7.76	10.05	
23 Mar 2004	0.243	7.71	0.0061	0.14	1.34	1.50	0.304	8.18		
24 May 2004	0.233	7.62	0.0048	0.12	1.35	1.24	0.282	7.55		
	Days	Na	K	Ca	Mg	Mn	Fe	NH_3-N	Al	Ba
Karlsruhe ISM-S Tracer Test 2										
1 Jun 2004	0	8.83	0.14	2.62	1.71	0.014	0.00020	0.00528	<0.0019	0.0025
19 Jul 2004	48	8.00	0.14	2.45	1.59	0.015	<0.00018	<0.00071	<0.0019	0.0027
13 Sep 2004	104	7.13	0.14	2.31	1.52	0.015	<0.00018	<0.00071	<0.0019	0.0025
26 Oct 2004	147	7.05	0.15	2.37	1.56	0.015	0.00041	<0.00071	<0.0019	0.0026
6 Dec 2004	188	6.18	0.14	2.22	1.45	0.014	<0.00018	<0.00071	<0.0019	0.0032
3 Feb 2005	247	5.87	0.14	2.23	1.43	0.014	0.00023	<0.00071	0.0033	0.0023
12 Apr 2005	315	5.70	0.14	2.27	1.47	0.015	0.00032	<0.00071	<0.0019	0.0023
14 Jun 2005	378	5.39	0.14	2.29	1.48	0.014	0.00038	0.00214	<0.0019	0.0024
2 Aug 2005	427	4.92	0.14	2.18	1.38	0.014	0.00079	<0.00071	<0.0019	0.0023
22 Sep 2005	478	4.57	0.13	2.09	1.34	0.013	<0.00018	0.00757	<0.0019	0.0022
	SiO_2	pH	F	Cl	SO_4	NO_3^-—N	Br	Inorg C	$\delta^{15}N$	
1 Jun 2004	0.359	7.33	0.0048	0.14	1.43	7.05	0.745	7.48	0.92	
19 Jul 2004	0.310	7.57	0.0058	0.15	1.28	5.93	0.635	7.77		
13 Sep 2004	0.281	7.40	0.0058	0.14	1.42	5.76	0.624	7.51	4.08	
26 Oct 2004	0.263	7.40	0.0053	0.14	1.47	4.52	0.544	7.94		
6 Dec 2004	0.253	7.66	0.0057	0.13	1.45	3.47	0.476	7.83	8.87	
3 Feb 2005	0.243	7.59	0.0051	0.13	1.46	2.45	0.382	7.88		
12 Apr 2005	0.240	7.66	0.0056	0.13	1.48	1.96	0.354	7.78	11.92	
14 Jun 2005	0.243	7.69	0.0052	0.13	1.52	1.56	0.312	7.92		
2 Aug 2005	0.233	7.72	0.0049	0.13	1.61	1.33	0.298	7.84		
22 Sep 2005	0.221	7.49	0.0056	0.12	1.47	0.91	0.233	7.83	15.97	

[a] No denitrification detected; data were not considered for modeling of e^- donor contributions.

We desired to use a range of e^--donating Fe(II)-bearing minerals such that they, and denitrification reactions simulated with them, were consistent with the XRD, Mössbauer, and water quality data measured and provided a reasonable minimum-to-maximum envelope of the amount of denitrification contributed by non-pyritic Fe(II). The potential Fe(II)-bearing minerals detected, other than pyrite, which will be considered below as a source of inorganic sulfide, were clinochlore, biotite, and amphibole. Neither clinochlore [$(Mg,Fe^{2+})5Al(Si_3Al)O_{10}(OH)_8$] nor biotite [$K(Mg,Fe^{2+})_3(Al,Fe^{3+})$-$Si_3O_{10}(OH)_2$] has equal proportions of Ca and Mg; furthermore, reactions with biotite would produce K, which did not increase in the ISMs. Therefore, we chose two amphiboles to provide an estimate of the range of Fe(II) that contributed to denitrification. The data on Table 2 show small increases in F, particularly for the two tracer test in ISM-S, which may indicate hornblende reactivity. Therefore, hornblende was added as an e^- donor to PHREEQC as a "minimized" source of Fe(II). It had 1.5 mol of Fe(II), it had equal proportions of Ca and Mg (2 mol each/mol hornblende), and it had an Fe(II) fraction of 60%, which was within the range determined by Mössbauer spectroscopy:

$$Ca_2Mg_2Fe_{2.5}Si_8O_{22}(OH)_2 + 14H^+ + 8H_2O \leftrightarrow 2Ca^{2+} + 2Mg^{2+} + 1.5Fe^{2+} + 1Fe^{3+} + 8H_4SiO_4 \quad (2)$$

A hypothetical "mixed-Fe" amphibole was added to PHREEQC as a "maximized" source of Fe(II). It had 4 mol of Fe(II) per mol, it had no Ca and Mg, and it had Fe(II) at the upper limit of the range given by Mössbauer spectroscopy:

$$Fe_6Si_8O_{22}(OH)_2 + 14H^+ + 8H_2O \leftrightarrow 4Fe^{2+} + 2Fe^{3+} + 8H_4SiO_4 \quad (3)$$

The reaction in the phreeqc.dat database for the oxidation of Fe(II) is:

$$Fe^{2+} \leftrightarrow Fe^{3+} + e^- \quad (4)$$

The reactions in the phreeqc.dat database for the oxidation of pyrite involve a set of equations,

$$FeS_2 + 2H^+ + 2e^- \leftrightarrow Fe^{2+} + 2HS \quad (5)$$

and

$$HS^- + 4H_2O \leftrightarrow SO_4^{2-} + 9H^+ + 8e^- \quad (6)$$

plus Reaction (4). Adding Reactions (4)–(6) yields

$$FeS_2 + 8H_2O \leftrightarrow 2SO_4^{2-} + Fe^{3+} + 16H^+ + 15e^- \quad (7)$$

for which 14/15 of the electrons provided are from the oxidation of sulfide and 1/15 are from the oxidation of Fe(II). The half-reactions shown by Reactions (4) and (7) were reacted with the following nitrate reduction half-reaction in PHREEQC:

$$2NO_3^- + 12H^+ + 10e^- \leftrightarrow N_2 + 6H_2O \quad (8)$$

PHREEQC brings all of the products in these reactions to thermodynamic equilibrium with the analytes in the modeled water samples.

The third step involved reacting the modified initial sample analytical data with the e^- donors defined above to determine which mix of donors best explained the pH and concentrations of inorganic C, Ca, and Mg measured in the subsequent sample. Denitrification by pyrite was considered the simplest to quantify because it produces sulfate (Reaction (7)). Sulfate is believed to be conservative because nitrate was always in the water, and denitrification is more energetic than sulfate reduction (Korom, 1991), and because major sulfate minerals were undersaturated in the ISMs (a result to be discussed below). Therefore, any increase in measured sulfate was attributed to denitrification and the amount of denitrification involved was determined stoichiometrically from Reactions (7), (8). Each mol of sulfate produced was assumed to be a result of 3/2 mol of nitrate reacting with 1/2 mol of pyrite. The remainder of the nitrate lost, with respect to the Br tracer, was attributed to the oxidation of OC (Reaction (1)) and the oxidation of Fe^{2+} [Reaction (4)] produced by Reactions (2), (3).

After simulating denitrification by pyrite in PHREEQC, the following three additional scenarios were also simulated in PHREEQC on any remaining denitrification detected in the ISMs:

(1) by OC only;
(2) by equal amounts (stoichiometrically) of OC and mixed-Fe amphibole; and
(3) by 90% OC and 10% hornblende.

After simulating denitrification for each sampling event with the suite of e^- donors described above, the fourth and final step equilibrated the simulated water with calcite, magnesite, and quartz to force the simulated water to have the same SI values for these minerals as the actual water sample. Not all the products of denitrification reactions are conservative in groundwaters in the ISMs. For example, research at another ISM site (Korom et al., 2005) suggested that magnesian calcite precipitated from solution during denitrification in an ISM. To simulate the possibility that inorganic C produced via Reaction (1) may have been lost from solution as magnesian calcite, the simulated solution was forced to the same SIs values for calcite and magnesite as the actual water. Likewise, to simulate the possibility that silicic acid produced via Reactions (2), (3) may have been lost from solution, the simulated solution was forced to the same SI for quartz as the actual water.

Steps 1–4 were repeated for each successive sampling date after the initial sample. This modeling methodology forced exact matches between simulated and actual dissolved concentrations for sulfate, nitrate, and Br and resulted in an exact match for silica and an approximate match for Na. K, Mn, Fe, ammonium, Al, Ba, F, and Cl concentrations changed little during the tracer tests (Table 2), so these analytes were judged to play minor roles in the denitrification reactions. The remaining four analytes, pH, IC, Ca, and Mg, were monitored to see which mix of e^- donors best explained the evolution of these analytes with denitrification in the ISMs.

2.4. Multiport samplers

Due to several factors, including recharge through the vadose zone, dispersion, and denitrification, groundwater nitrate concentrations are commonly stratified with the largest concentrations near the water table. To characterize the stratified conditions, twelve MPSs, adapted from the design of Pickens et al. (1978), were installed in the aquifer in 2001. The MPSs were placed using a hollow-stem auger, and the natural formation was collapsed as the auger was lifted. Sampler depths, with reference to the water table (bwt), were about 0, 0.6, 1.2, 1.8, 2.4, 3.0, 4.6, 6.0, and 9.1 m bwt (allowing for water table fluctuations of up to 1.2 m). Freezing temperatures in North Dakota from the end of October through the middle of April essentially eliminate recharge through the frost zone. Therefore, the MPSs were sampled during this period to monitor nitrate concentrations for evidence of denitrification without having to consider intermixing with nitrate coming from the vadose zone. During the fall and winter of 2001/2002, the MPSs and one well nest were used to monitor apparent reductions in nitrate concentrations using a mass balance approach and to estimate denitrification rates. During the fall and winter of 2003/2004, five of the MPSs were used for isotope analysis of ^{15}N and ^{18}O; the purpose being to determine if isotopic enrichment in the remaining nitrate supported the hypothesis that denitrification explained the nitrate losses noted in some of the MPS samples in the study done 2 year earlier (Spencer, 2003). In addition, the isotopes would be used to determine whether the predominant source of nitrate in the Karlsruhe Aquifer was, indeed, from fertilizer.

For the isotopic study conducted during the fall and winter of 2003/2004, sites were selected using the following criteria:

(1) that they represented the variability of the aquifer (Fig. 2); and
(2) that they had sufficient nitrate concentrations in the preliminary samples to allow for isotope analysis.

Sample depths ranged from 1.5 to 10.4 m below the land surface. All wells were initially purged to assure collection of representative formation water. Water samples were collected on 21 October 2003, 22 December 2003, and 22 March 2004, sterilized with a saturated HgCl solution (1 drop solution per 100 mL of sample), and refrigerated until isotopic analysis. Twenty groundwater samples from the MPSs were sent to the Environmental Isotope Laboratory at the University of Waterloo, Ontario, Canada, for isotope analysis of $\delta\ ^{15}N$ and $\delta\ ^{18}O$ in nitrate using mass spectroscopy (Flatt and Heemskerk, 1997).

2.5. Mass Balance Computations

During the fall and winter of 2001–2002, local denitrification rates were estimated at MPS sites, for which isotopic data indicated substantial denitrification, using a mass balance method. The mass balance method assumed that all nitrate loss was caused by denitrification. To reasonably assume this, the site must have the following attributes:

(1) be approximately isotropic with respect to nitrate in the lateral direction within the effective length of groundwater flow during the study period (defined below);
(2) have negligible nitrate influx from the surface, or loss through the bottom boundary of the measured unit; and
(3) have negligible dilution from surficial influx of water over the period of measurement.

With such requirements and assumptions, the rigor of the mass balance method and confidence in denitrification rate estimates are lower than that of the ISMs. They are of interest, however, for comparison with the ISM results, which are more costly to obtain, and as a potential method for evaluating situations where ISM data are unavailable. Furthermore, the mass balance method may be used to measure ambient nitrate losses and serve, therefore, to complement the amended denitrification measurements in the ISMs. There are several measures in the treatment of the mass-balance data that may be used to minimize potential error.

For a first-order denitrification rate, identifying the initial concentration is important. However, determining an initial nitrate concentration is problematic for a stratified nitrate profile where the highest concentrations are usually located within the upper profile, which is closer to the entry boundary and which is usually more oxidized. Nitrate reduction processes within the stratified profile must be viewed as dynamic, with denitrification occurring predominantly in the lower and unoxidized portion of the profile, and with nitrate diffusing toward the zone of denitrification within that profile. Where the unoxidized zone is caused by greater concentrations of reduced minerals from slower historical weathering, temporary fluctuations in the water table may also serve to draw surficial nitrates deeper and into closer proximity to the reducing zone. To minimize these problems, we chose to use a total profile mass balance for estimation of denitrification rates. By integrating all stratified concentrations over depth to the point of nitrate extinction, Z_f, the depth-averaged concentration at any time is

$$\bar{C}_t = \frac{\int_0^{Z_f} C_z dz}{Z_f} \quad (9)$$

where C_z is the nitrate-N concentration at depth z, we avoid the possibility of boundary losses and eliminate potential problems of dilution through additional water influx because, regardless of concentration at any given depth, the total mass of nitrate is accounted for within the profile.

We chose to use the integrated mean concentration for the profile (Eq. (9)) as our metric to avoid errors resulting from misinterpretation of depth-specific nitrate dynamics within the profile. For common horizontal water-table gradients (0.0002–0.0004 for the Karlsruhe aquifer), an effective porosity of about 0.2, and a range of hydraulic conductivity values from about 30–60 m/d, the annual lateral distance of effect would be about 12–50 m. For widespread contamination caused by non-point source pollution, and from 9 years of monitoring the aquifer, we believe that lateral isotropy should be reasonably approximated within this effective length. To avoid surficial influx of nitrate, the winter period, which is characterized by frost up to 2 m deep in North Dakota from October to April, was used for all measurements, with one exception, as noted below. Sites were chosen that exhibited decreasing nitrate over that time period and no further vertical expansion of the contaminant zone. Groundwater samples for both fall-winter sampling schedules were filtered and analyzed with the same methods used for the ISMs described earlier.

3. Results and discussion

The results from the analyses of the aquifer sediment samples, the ISMs, the geochemical modeling, the multiport samplers, and the mass balance computations are provided and discussed below.

3.1. Aquifer sediment samples

Stratified sediment samples collected during construction of the MPSs (Table 1) indicated that potential electron donors were highly variable and generally low (H. Durbin, written communication, 3 August 2001). Five of 21 sediment samples had no measurable sulfide-S. The sixteen samples with detections of sulfide-S were normally distributed, had a median value of 0.05% (sediment dry wt.), a mean of 0.064%, a standard deviation of 0.047%, and a maximum of 0.18%. Values for TOC were log-normally distributed, ranging from 0.01% to 0.93%, with a median of 0.05%.

Analysis of sediment samples collected from the ISM-G site by Tesfay (2006) indicated that sediments contained 0.25 ± 0.082% sulfide (±1 standard deviation), 0.051 ± 0.024% OC, and 0.24 ± 0.31% amorphous Fe(II). The ISM-S sediments contained 0.19 ± 0.074% sulfide, 0.017 ± 0.009% OC, 0.23% amorphous Fe(II) and 0.49% total Fe(II). The ISM-G and ISM-S e^--donor results were larger than the median values determined for the seven MPS sites (Table 1) for sulfide, and the ISM-G results were greater than ISM-S for TOC. The amorphous Fe(II) results were similar for both ISM sites. The ISM-S sediments were finer than those at the G-ISM site. At the G site the sediments were 25% gravel, 71% sand, 0% silt, and 4% clay; at the S site the sediments were 9% gravel, 88% sand, 0% silt, and 3% clay.

For comparison of the e^- donor concentrations, sediment samples taken below the water table in the Elk Valley aquifer in eastern ND, which has detrital shale fragments in it, may have >1% sulfide-S (Schuh et al., 2006) and had average TOC concentrations >0.4% (Kammer, 2001; Tesfay, 2006).

3.2. In Situ Mesocosms

Figs. 3 and 4 present the results for denitrification rates and the isotopic enrichment of ^{15}N remaining in the ISMs, respectively.

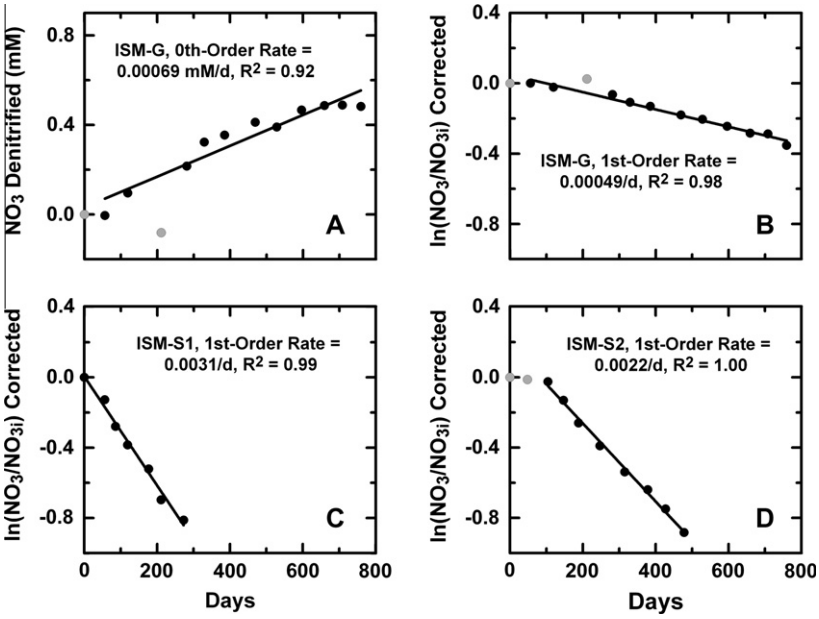

Fig. 3. Denitrification rates measured in the in situ mesocosms (ISMs). A. ISM-G, zero-order rate; B. ISM-G, first-order rate; C. ISM-S, first tracer test, first-order rate; and D. ISM-S, second tracer test, first-order rate. Only black data points were used in the linear regressions.

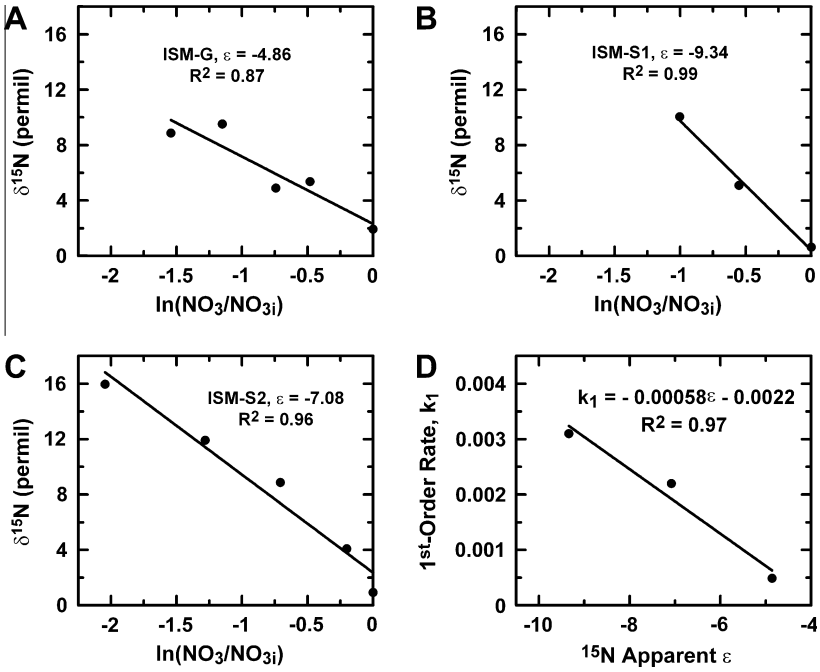

Fig. 4. Isotopic enrichment of ^{15}N in the residual nitrate in the ISMs (A–C) and the apparent linear relationship between the measured first-order denitrification rates and apparent ^{15}N enrichment.

Figs. 5 and 6 show the model results of the geochemical analyses for the amounts of denitrification caused by the suite of e^- donors.

3.2.1. Denitrification rates

A zero-order regression model for denitrification in ISM-G (after adjustment for dilution using Br as a tracer) is shown on Fig. 3A. Composite data indicated an approximate linear denitrification rate of 0.00069 mM/d ($R^2 = 0.92$). However, the data for the first 211 d exhibited little denitrification, possibly due to the initial disturbance during construction, where some oxygenation may occur through oxidized drilling fluid. Unpublished research by J. Gallagher of the Energy and Environmental Research Center at the University of North Dakota indicated that a long-term recovery period (>1 year) was required for initiation of autotrophic denitrification in isolated laboratory chambers using disturbed and partially aerated sediment samples from the Elk Valley aquifer (written communication, J. Gallagher, 1995). For this reason measurements were continued for 759 d. Omitting the first and fourth data points, denitrification is best fit using a first-order function, which is concentration-dependent:

$$C_t = C_0 e^{-kt} \tag{10}$$

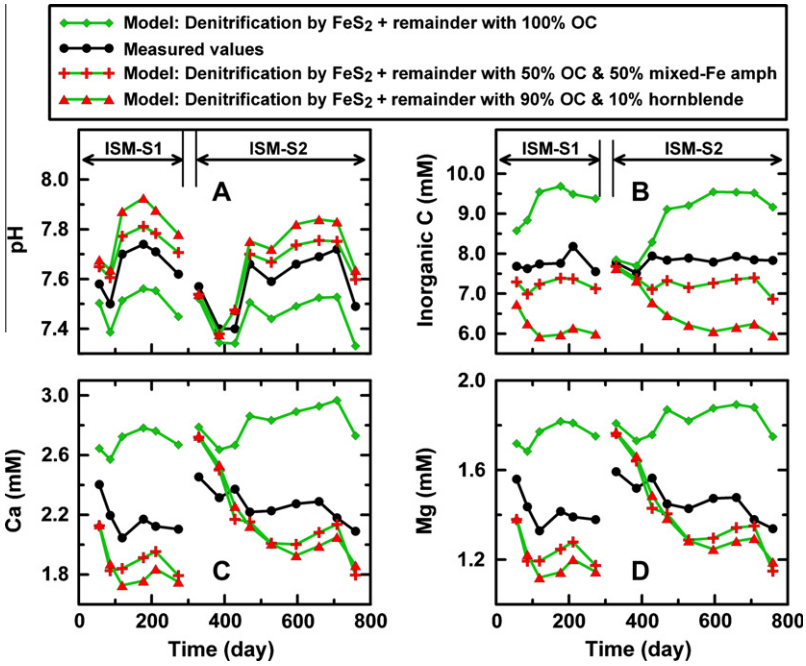

Fig. 5. Model results for the e^- donors contributing to the denitrification measured in the two tracer tests in ISM-S. The resulting values for pH (A), inorganic C (B), calcium (C), and magnesium (D), compared to the actual values, for denitrification caused by pyrite with the remaining denitrification caused by 50% organic C + 50% mixed-Fe amphibole or with the remaining denitrification caused by 90% organic C + 10% hornblende.

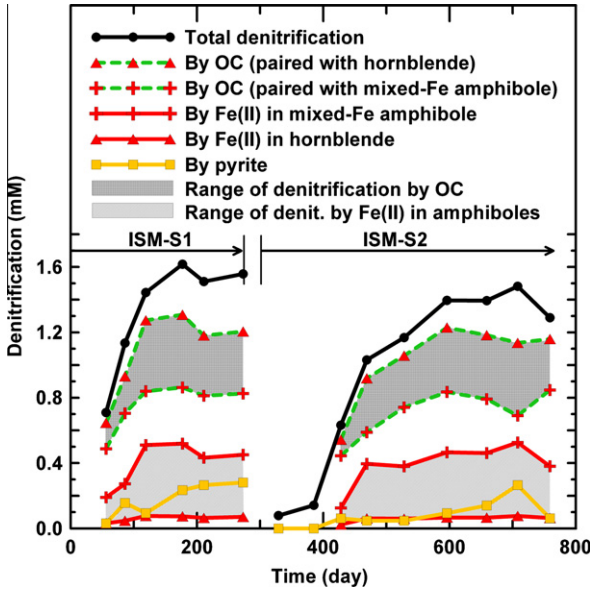

Fig. 6. The amounts of denitrification caused by pyrite, organic C, and Fe(II) in mixed-Fe amphibole or in hornblende, as calculated from the results shown on Fig. 5.

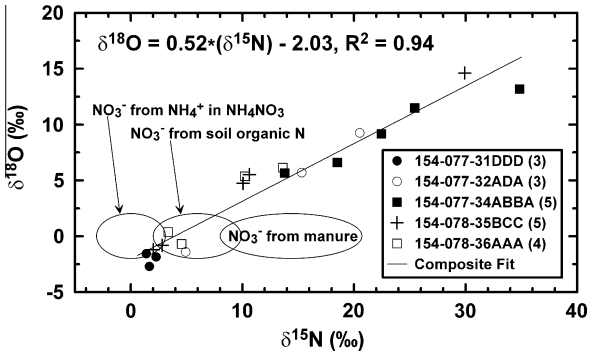

Fig. 7. The enrichment of ^{18}O vs. ^{15}N for the residual nitrate at five multiport groundwater monitoring sites. Isotope ranges for fertilizer, soil organic matter, and manure are from Mengis et al. (2001).

where C_0 is the initial concentration, C_t is the concentrations after time, t, and k = 0.00049/d (R^2 = 0.98). The linear fit of the first-order rate is shown on Fig. 3B.

Two tracer tests were conducted in ISM-S, the first for 273 d and the second for 478 d. Like for ISM-G, denitrification was better modeled as a first-order reaction. For ISM-S1 the first-order rate was 0.0031/d with R^2 = 0.99 (Fig. 3C), compared with a zero-order rate of 0.0055 mM/d, R^2 = 0.75 (not shown), and for S2 the first-order rate was 0.0022/d with R^2 = 1.00 (Fig. 3D), compared with a zero-order rate of 0.0029 mM/d, R^2 = 0.71 (not shown).

All three denitrification tracer tests in the Karlsruhe Aquifer ISMs showed denitrification to be better modeled as a first-order reaction. Most published aquifer denitrification rates appear to be reported as zero-order reactions (Korom, 1992, and references therein; Green et al., 2008, Fig. 8 and references therein), which makes direct comparisons difficult with our results. However using the less-accurate zero-order rates for the Karlsruhe ISMs, they would plot near the median value of the zero-order denitrification rates for the 23 sites summarized in Fig. 8 in Green et al. (2008). Compared (again using the less-accurate zero-order rates) to another ISM site in eastern North Dakota, for which denitrification was better explained by a zero-order rate, the Karlsruhe denitrification rates were 2.9 (for ISM-S1) to 23 (for ISM-G) times slower (Korom et al., 2005).

In laboratory studies Arah (1990) noted that first-order denitrification rates occur for lower nitrate concentrations than observed in the ISMs. This suggests that something influenced the availability of the e^- donors or otherwise restricted denitrification reactions in the Karlsruhe ISMs. Processes that may have influenced

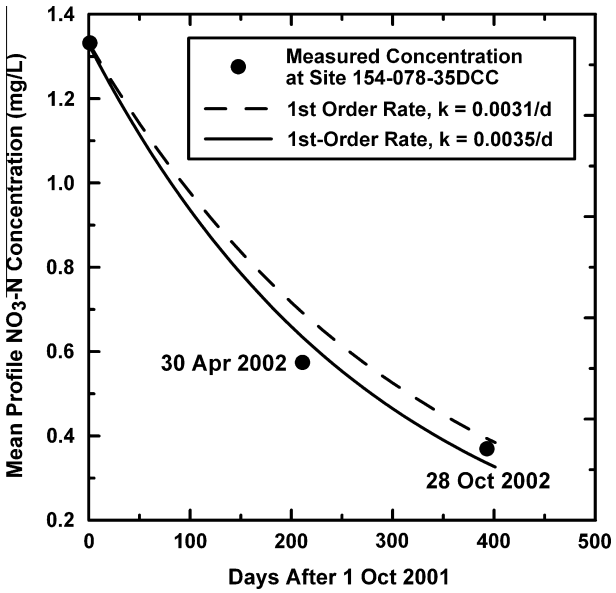

Fig. 8. Comparison of nitrate dissipation data with a first-order reaction rate calculated using the k value measured from the first tracer test in ISM-S (solid line) and a k value providing a better fit (dashed line).

denitrification rates in the ISMs may also have influenced field measurements of apparent isotopic enrichment factors, ε; these processes are discussed below for both rates and ε values.

3.2.2. Enrichment of ^{15}N

That denitrification in the ISMs explained the loss of nitrate relative to Br was evidenced by the enrichment of ^{15}N in the remaining nitrate. Fig. 4 shows the ε values for the ISM tracer tests. For ISM-G, $\varepsilon = -4.86‰$ ($R^2 = 0.87$); for ISM-S1, $\varepsilon = -9.34‰$ ($R^2 = 0.99$); and for ISM-S2, $\varepsilon = -7.08‰$ ($R^2 = 0.96$. Mariotti et al. (1982) found in lab experiments using soils with nitrite as a substrate, that there was an exponential relationship between ε and first-order denitrification rates (ε vs k_1), with greater enrichment (more negative ε) associated with the slower rates. Our results (Fig. 4D), plotted as k_1 vs. ε, because knowing ε would allow for an estimate of k_1, show a linear fit ($R^2 = 0.97$) with greater enrichment associated with faster rates. The reasons for the disparity between our relationship and that found by Mariotti et al. (1982) are unknown, but they may be associated with discrepancies noted between lab-based studies and those done in the field.

The mean value of ε for the three ISM tracer tests is $-7.09‰$. This value is in the interquartile range for groundwater values reported by Green et al. (2010, Fig. 11d), but less (less negative) than the median laboratory culture value of about $-19‰$. Thus, both the first-order rates of denitrification and the isotopic fractionation in the ISMs are lower than lab estimates. On this issue Green et al. (2010, p. 12) noted that "physical mixing tends to create the appearance of lower reaction rates and fractionation parameters when measured at larger scales and longer flow paths." Kawanishi et al. (1993) reported that dispersion decreases the apparent N isotope fractionation. However, the ISMs were designed to minimize advection and mechanical dispersion; thus, the influence of these processes on denitrification rates and fractionation of the nitrate placed inside the ISMs should be minimal. At the first site ISMs were used (Korom et al., 2005), measurements (using a similar ISM design and tracer test methodology) showed zero-order denitrification with $\varepsilon = -20.4‰$; the latter being comparable to the median "simulated true" ε value reported by Green et al. (2010, Fig. 11d). We speculate that reaction rates and ε values found in the ISMs may be more representative of local aquifer conditions than lab-based estimates or estimates measured along aquifer flowpaths. Our ISMs are large enough to incorporate denitrification microsites, which are differentially distributed in soil aggregates at scales larger than most lab-based studies (Arah, 1990), and they minimize the hydrodynamic mixing associated with larger flow-path measurements (Kawanishi et al., 1993; Green et al., 2010).

Both the ISMs and the MPSs allow the analysis of relatively localized conditions, compared to flow-path studies, which may be why the denitrification rates measured both ways agree reasonably well with each other, as discussed below. Unfortunately, data limitations for the MPSs do not allow similar comparisons of ε values to those for the ISMs.

3.3. Geochemical modeling

Of the three types of electron donors considered herein, denitrification by sulfide (as pyrite at Karlsruhe) is believed to be the most straightforward to track because the sulfide product of sulfate [Reaction (7)] appears to have been stable in the ISMs. Table 3 shows the solution SIs for barite, gypsum, epsomite, and jarosite-K in water samples collected from the ISMs. Only barite is supersaturated; however, the data for dissolved barium on Table 2 show that the greatest range between the maximum and minimum barium concentrations for any tracer test was 0.0010 mM (ISM-S2). Such a small decrease in barium, if a result of barite precipitation, would correspond to an insignificant loss of sulfate. Furthermore, with plenty of nitrate in the water, sulfate reduction would not be expected to be a significant redox reaction in the ISMs (Korom, 1991). For the non-sulfate minerals, calcite SIs were near equilibrium, or slightly supersaturated, during the ISM tracer tests; quartz was slightly supersaturated, and magnesite was at or below saturation.

Simulated pH values resulting from the various electron-donor contribution scenarios for the ISM-S1 and S2 tracer tests using PHREEQC are shown on Fig. 5A. ISM-G results (not shown) were not distinct, much like the early part of the ISM-S2 results (Fig. 5A). Furthermore, the first two datum points of ISM-S2 and all the data for ISM-G were associated with low denitrification rates; apparently too low to allow for definitive interpretation of the various e^--donating scenarios. Therefore ISM-G results, as well as those for the first two datum points for ISM-S2, are not discussed further.

The pH results show that the measured values cannot be matched merely by the denitrification of pyrite (to explain the increases in sulfate) and OC. There must be some denitrification by Fe(II) to reproduce the measured pH values. The measured values are about half way between the simulated results using denitrification by pyrite (to explain the increase in sulfate) and the line representing the rest of the denitrification by OC and the line representing the rest of the denitrification by 90% OC and 10% hornblende. Therefore, the measured values are approximately simulated with denitrification by pyrite to explain the increases in sulfate, with the remainder of the denitrification produced by a mix of 95% OC and 5% hornblende. This relationship is roughly valid for both tracer tests in ISM-S (Fig. 5A). Similarly the measured values could also be reproduced with denitrification by pyrite, with the remainder of the denitrification produced by a mix of about 65% OC and 35% mixed-Fe amphibole. Thus, the approximate range of contribution of Fe(II) to denitrification in the ISM-S tests, after denitrification by pyrite to explain the increases in sulfate, was about 5%, if the Fe(II) was provided by hornblende (as modeled herein), to about 35%, if the Fe(II) was provided by minerals simulated as our "mix-Fe" amphibole. Figs. 5B–D show that these proportions are roughly similar for measured inorganic C, Ca, and Mg concentrations, respectively, as well.

Table 3
Saturation indices for the dissolved ion data measured for water samples collected in the in situ mesocosms given in Table 2.

Date	Barite	Gypsum	Epsomite	Jarosite-K	Calcite	Magnesite	Quartz
Karlsruhe ISM-G							
25 Aug 2003	0.50	−2.12	−4.38	−8.73	0.25	−0.29	0.76
20 Oct 2003	0.48	−2.13	−4.38	−6.64	0.49	−0.04	0.76
22 Dec 2003	0.43	−2.16	−4.43	−7.44	0.53	−0.02	0.73
23 Mar 2004	0.52	−2.13	−4.41	−6.93	0.67	0.11	0.76
1 Jun 2004	0.54	−2.08	−4.35	−7.94	0.29	−0.27	0.73
19 Jul 2004	0.57	−2.10	−4.37	−7.03	0.79	0.24	0.73
13 Sep 2004	0.54	−2.08	−4.35	−7.62	0.29	−0.25	0.73
6 Dec 2004	0.68	−2.07	−4.34	−9.80	0.01	−0.54	0.73
3 Feb 2005	0.52	−2.09	−4.36	−6.98	0.49	−0.06	0.73
12 Apr 2005	0.54	−2.06	−4.33	−7.85	0.35	−0.20	0.73
14 Jun 2005	0.56	−2.05	−4.32	−6.15	0.69	0.15	0.74
2 Aug 2005	0.57	−2.05	−4.32	−5.00	0.63	0.08	0.72
22 Sep 2005	0.54	−2.08	−4.35	−5.84	0.57	0.02	0.72
Karlsruhe ISM-S Tracer Test 1							
25 Aug 2003	1.13	−1.53	−4.05	−7.16	0.41	−0.39	0.76
20 Oct 2003	1.11	−1.54	−4.07	−7.13	0.41	−0.40	0.68
19 Nov 2003	1.15	−1.53	−4.05	−6.30	0.29	−0.51	0.62
22 Dec 2003	1.05	−1.56	−4.09	−6.73	0.48	−0.32	0.58
18 Feb 2004	1.19	−1.51	−4.03	−6.09	0.55	−0.26	0.60
23 Mar 2004	1.13	−1.51	−4.03	−6.62	0.53	−0.27	0.59
24 May 2004	1.14	−1.50	−4.02	−5.99	0.40	−0.40	0.57
Karlsruhe ISM-S Tracer Test 2							
1 Jun 2004	1.15	−1.45	−3.97	−7.92	0.15	−0.65	0.76
19 Jul 2004	1.15	−1.51	−4.03	−7.16	0.40	−0.40	0.70
13 Sep 2004	1.17	−1.47	−4.00	−7.79	0.18	−0.61	0.65
26 Oct 2004	1.19	−1.45	−3.97	−6.52	0.22	−0.58	0.62
6 Dec 2004	1.30	−1.47	−3.99	−6.72	0.47	−0.33	0.61
3 Feb 2005	1.15	−1.46	−3.99	−6.42	0.40	−0.41	0.59
12 Apr 2005	1.16	−1.44	−3.97	−5.76	0.48	−0.33	0.58
14 Jun 2005	1.19	−1.43	−3.96	−5.47	0.52	−0.28	0.59
2 Aug 2005	1.19	−1.42	−3.96	−4.39	0.53	−0.29	0.57
22 Sep 2005	1.17	−1.46	−4.00	−7.28	0.28	−0.53	0.55

Fig. 6 shows the approximate denitrification contributions of the three e^- donors [pyrite, OC, and non-pyrite Fe(II)] modeled for the Karlsruhe ISM data. The lines for Fe(II) and OC are averages of linear interpolations between the lines discussed above for Fig. 5 for pH, IC, and Ca. The Ca and Mg results produced essentially the same proportions, so only results for Ca were used in calculating the averages. The variation in the linearly-interpolated values provided by pH, IC, and Ca data was small. For example, the fourth data point for the line representing denitrification by OC paired with hornblende, which corresponds to the greatest amount of denitrification measured for either tracer test, was 1.280 mM for pH, 1.283 mM for IC, and 1.258 mM for Ca, for an average value of 1.274 mM.

The simulations represented on Fig. 6, depending on the sample date, indicate that in ISM-S1, pyrite was the apparent e^- donor for 4–18% of the denitrification [with 14/15 by sulfide and 1/15 by Fe(II)]; the range for Fe(II) was 3–6% as hornblende to 22–37% as mixed-Fe amphibole; the range for OC was 77–91% when paired with hornblende to 49–73% when paired with mixed-Fe amphibole. For ISM-S2, the contributions by pyrite were the same as for ISM-S1; the range for Fe(II) was 2–8% as hornblende to 13–43% as mixed-Fe amphibole; the range for OC was 75–92% when paired with hornblende to 43–68% when paired with mixed-Fe amphibole. To our knowledge, this is the first time modeling results have been reported for relative contributions to denitrification by the three major e^- donors.

Aquifer denitrification rates for OC and pyrite e^- donors are more commonly reported in the literature than is nitrate reduction by Fe(II) (Korom, 1992, and references therein; Green et al., 2008, Fig. 8 and references therein). An exception is provided by Postma (1990), who studied the kinetics of denitrification by detrital Fe(II)–silicates. Using a fluidized bed reactor with arfvedsonite

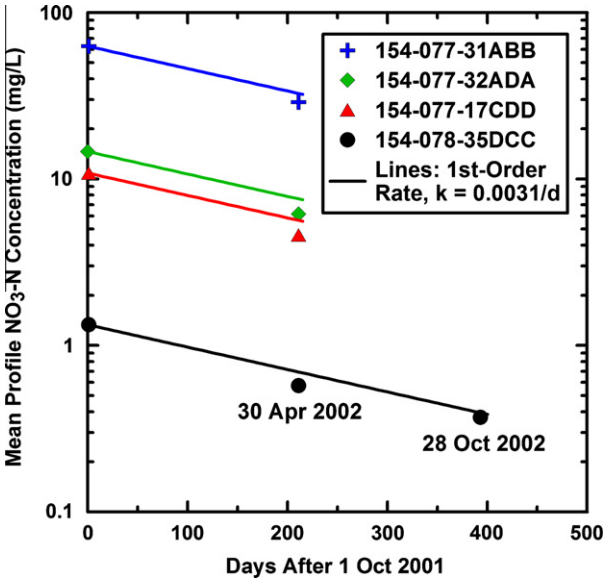

Fig. 9. Measured nitrate dissipation rates for MPS data and predicted nitrate dissipation rates using a first-order reaction rate with the k value measured from the first tracer test in ISM-S (0.0031/d). Site 154-077-31ABB is a well nest of six wells.

$[Na_3(Fe^{2+},Mg)_4Fe^{3+}Si_8O_{22}(OH)_2]$ as an example for amphiboles and augite $[(Ca,Na)(Mg,Fe,Al)(Si,Al)_2O_6]$ for pyroxenes, he estimated zero-order nitrate reduction rates of "roughly" 4×10^{-5} M/year for these minerals (Postma, 1990, page 903). For comparison purposes, the approximate zero-order rates for ISM-S1 and ISM-S2,

Table 4
Calculated first-order nitrate dissipation rates calculated from MPS data.

Site USBR nomenclature	Sample period (d/m/y)	C_0 (mg/L)	C_t (mg/L)	k (Eq. (10)) (d^{-1})
154-077-17CDD	1/10/2001-30/4/2002	10.9	4.60	0.00407
154-077-31ABB[a]	1/10/2001-30/4/2002	62.8	29.0	0.00367
154-077-32ADA	1/10/2001-30/4/2002	14.6	6.15	0.00410
154-078-35BCC	22/10/2003-9/4/2004	42.4	26.5	0.00276
154-078-35DCC	1/10/2001-30/4/2002	1.33	0.574	0.00399
154-078-35DCC	1/10/2001-28/10/2002	1.33	0.370	0.00327

[a] This site is a well nest of six wells.

after conversion, were 2.0×10^{-3} M/year and 1.1×10^{-3} M/year, respectively. Multiplying each value by the respective contribution range of Fe(II) in hornblende provided by our geochemical model for ISM-S1 (3–6%) and ISM-S2 (2–8%) provides a low rate of 2.2×10^{-5} M/year and a high rate of 1.3×10^{-4} M/year for nitrate reduction by Fe(II) in hornblende, which bracket Postma's value. For our mixed-Fe amphibole simulations the Fe(II) denitrification rates were 1.4×10^{-4} M/year to 7.3×10^{-4} M/year, which are about an order of magnitude more than Postma's rate.

Previously it was noted that hydrogeological complexity (''mixing'') influences field denitrification rates so that they are unlikely to match those measured under laboratory conditions (Green et al., 2010). The ISMs reduce this complexity by essentially eliminating advection and mechanical dispersion processes. Nevertheless, it is possible that the similarity between Postma's (1990) lab rates and the ISM rates for nitrate reduction by Fe(II) in hornblende is coincidental.

3.4. Multiport samplers

Determination of ^{18}O and ^{15}N in nitrate can help determine its sources as well as the presence of denitrification. The predominant sources of fertilizer used by growers in the Karlsruhe area are anhydrous ammonia and urea, both of which form ammonium in water. In aerated soils, ammonium is normally nitrified by bacteria to form nitrate within a few days of application. An additional supplemental fertilizer form, used for foliar application through the irrigation system, is 28% solution UAN (dissolved urea + ammonium nitrate) and therefore contains a small amount of nitrate. Using $\delta\ ^{18}O$ and $\delta\ ^{15}N$ ranges for NH_4NO_3, soil organic N, and manure from Mengis et al. (2001), the istope measurements shown on Fig. 7 are consistent with that expected for nitrified ammonium. Furthermore, the slope (0.52) of the $\delta\ ^{18}O$ vs. $\delta\ ^{15}N$ data for all sites is highly correlated ($R^2 = 0.94$), and agrees well with the expected enrichment ratio of 0.5 for denitrification (Kendall, 1998, and references therein). Site-by-site distributions of $\delta\ ^{15}N$ and $\delta\ ^{18}O$ vs. NO_3^-—N for the five MPSs chosen for isotope analysis are also shown on Fig. 7. Only the data from 154-073-31DDD shows no evidence of enrichment; groundwaters at the other sites appear to have been influenced by denitrification.

3.5. Mass balance computations

Of the five sites used to measure denitrification using the mass balance method, only one, 154-078-35DCC, was extended through the summer. An additional fall 2002 concentration was included for this site because continuing decreases in nitrate concentrations and overall low nitrate concentrations indicated that further influx of nitrate was unlikely during the growing season. The rate of nitrate loss for MPS 154-078-35DCC is shown on Fig. 8. As with both ISM sites, the dissipation data is better fit using a first-order model than a zero-order model. The first-order coefficient derived from ISM-S1, $k = 0.0031$/d, provides a reasonably good model for the MPS data. An improved fit using $k = 0.0035$/d is also plotted. All four other sites have only two data points, which is insufficient to determine whether a linear or first-order model is most appropriate. However, assuming the appropriateness of a first-order model, based on ISM and 154-078-35DCC MPS determinations, the remaining four sites were fitted using first-order models. Dissipation data for four of the five MPS sites are compared with predicted rates using $k = 0.0031$/d for each site on Fig. 9. Fits for all four sites are reasonably good. Best-fit first-order k values for each of the five sites are on Table 4. The mean k for the five mass balance measurement sites (using 154-078-35DCC with an ending date of 30 April 2002) is 0.00374/d ± 0.00056/d, with a confidence interval ($p < 0.05$) from 0.00302/d to 0.00442/d. The mean value does not differ significantly ($p < 0.05$) from the 0.0031/d k value measured in ISM-S1 (Fig. 3C).

4. Conclusions

Several strategies and methods were used to evaluate potential denitrification in an aquifer that had undergone extensive non-point source nitrate contamination. Analyses of OC and inorganic sulfide, as potential e^- donors, for 21 samples taken at various depths at seven multiport samplers (MPS) sites indicated that all but one site had at least one e^- donor present at a concentration >0.1%. In addition, two in situ mesocosms (ISMs) were placed in the reducing zone of the aquifer. Sediments from both ISM sites showed roughly similar concentrations of OC and inorganic sulfide as the MPS sites, as well as Fe(II) concentrations >0.2%.

Denitrification rates for tracer tests performed in the ISMs were best fit with a first-order kinetic model. One site (ISM-S1) had faster denitrification ($k = 0.0031$/d) in its first tracer test and a slightly lower rate in its second tracer test ($k = 0.0022$/d). Denitrification at ISM-G was non-measurable for the first 200 d. Thereafter, in an extended sample period to about 800 d, measurable denitrification did occur. As in ISM-S, the kinetic rate was first-order, but the rate was lower ($k = 0.00049$/d). ^{15}N data for water samples from both ISMs confirmed the occurrence of denitrification, with apparent enrichment factors of −4.86‰ for ISM-G, and −9.34‰ and −7.08‰ for the two successive tracer tests in ISM-S. First-order denitrification rate coefficients for both ISMs were found to be linearly related to the ^{15}N apparent enrichment factors. Relative e^- donor contributions for denitrification were modeled for both tracer tests conducted in ISM-S using PHREEQC and associated mineralogical and groundwater quality data. Results indicated that contributions to denitrification from individual election donors were about 4–18% from pyrite, 2–43% from non-pyrite Fe(II) in amphiboles, and 43–92% from OC, depending on the sample date. The models showed that denitrification by some non-pyrite Fe(II) was essential to explain the evolution of the groundwater quality parameters observed in ISM-S.

Isotopic analysis of ^{15}N vs ^{18}O for nitrate samples from five MPS sites indicated that denitrification was evident at four of them. Estimates of denitrification rates using a mass balance method for four other MPS sites and a well nest were fitted using first-order kinetic rates. Fitted k values for all five sites were similar to the

high denitrification rate at ISM-S (with $k = 0.0031$/d), with the range of k values for the mass balance method varying within a factor of two.

In general our work showed that, while nearly all sites showed some evidence of denitrification potential, seven of the 12 MPS sites, a well nest, and both ISM sites shown on Fig. 2 supported measureable denitrification. Barring more large-scale non-point releases of nitrate to the Karlsruhe aquifer, most areas of the aquifer appear to be able to naturally reduce nitrate concentrations to acceptable levels in the next couple of decades, assuming the rates measured herein are sustainable. However, some local areas may need additional remediation.

ISMs show promise for aquifer denitrification research at the local scale. They appear to be large enough to integrate the spatial variation caused by reactive microsites and they are designed to reduce mixing from advection and mechanical dispersion, which may influence values of kinetic rates and isotopic fractionation measured at large field scales. Modeling e^- donor contributions with the data provided by the ISMs helps determine what e^- donors are contributing to denitrification and at what rates. Coupling this knowledge with e^- donor concentrations available in sediments, and their associated reactivities, may provide insights on the long-term sustainability of denitrification reactions in aquifers.

Acknowledgments

The North Dakota Department of Health and the North Dakota State Water Commission (NDSWC) provided funding for this research. The North Dakota Water Resources Research Institute, funded by the US Geological Survey and NDSWC, provided a graduate research fellowship to E.J. Spencer. L. Charlet, Editor, B. Wehrli, Associate Editor, and two anonymous experts provided valuable assistance during the review process. A. Wanek, NDSWC, helped with the hydrologic interpretation of the Karlsruhe aquifer and J. Warne helped build and install the ISMs. We also thank the landowners that allowed us access to their land.

References

Arah, J.R.M., 1990. Modelling spatial and temporal variability of denitrification. Biol. Fertil. Soils 9 (1), 71–77.

American Society for Testing and Materials (ASTM), 1993. Construction, Section 04.08 Soil and Rock (I). Philadelphia, Pennsylvania, USA.

Bartelson, N., Goven, G., 1998. North Dakota Groundwater Monitoring Program 1998 Report. North Dakota Department of Health, Bismarck, ND, 143p.

Bates, H.K., Spalding, R.F., 1998. Aquifer denitrification as interpreted from in situ microcosm experiments. J. Environ. Qual. 27 (1), 174–182.

Böhlke, J.K., Denver, J.M., 1995. Combined use of groundwater dating, chemical, and isotopic analyses to resolve the history and fate of nitrate contamination in two agricultural watersheds, Atlantic coastal plain, Maryland. Water Resour. Res. 31 (9), 2319–2339.

Böhlke, J.K., Wanty, R., Tuttle, M., Delin, G., Landon, M., 2002. Denitrification in the recharge area and discharge area of a transient agricultural nitrate plume in a glacial outwash sand aquifer, Minnesota. Water Resour. Res. 38 (7). doi:10.1029/2001WR000663.

Burkart, M.R., Kolpin, D.W., 1993. Hydrologic and land-use factors associated with herbicides and nitrate in near-surface aquifers. J. Environ. Qual. 22 (4), 646–656.

Canfield, D.E., Raiswell, R., Westrich, J.T., Reaves, C.M., Berner, R.A., 1986. The use of chromium reduction in the analysis of reduced inorganic sulfur in sediments and shales. Chem. Geol. 54 (1–2), 149–155.

Churcher, P.L., Dickhout, R.D., 1987. Analysis of ancient sediments for total organic carbon – some new ideas. J. Geochem. Explor. 29 (1–3), 235–246.

Flatt, H., Heemskerk, A.R., 1997. $^{15}N/^{18}O$ in Dissolved Nitrate. Environmental Isotope Laboratory University of Waterloo Technical Procedure 12.0.

Frind, E.O., Duynisveld, W.H.M., Strebel, O., Boettcher, J., 1990. Modeling of multicomponent transport with microbial transformation in groundwater: the Fuhrberg case. Water Resour. Res. 26 (8), 1707–1719.

Gill, J.R., Cobban, W.A., 1965. Stratigraphy of the Pierre Shale, Valley City and Pembina Mountain Areas of North Dakota. US Geological Survey Professional Paper 392-A, 20p.

Gillham, R.W., Robin, M.J.L., Ptacek, C.J., 1990. A device for in situ determination of geochemical transport parameters 1. Retardation. Ground Water 28 (5), 666–672.

Golhaber, M.B., Kaplan, I.R., 1974. The sulfur cycle. In: Goldberg, E.D. (Ed.), The Sea, Marine Chemistry, vol. 5. John Wiley & Sons, New York, pp. 569–655.

Green, C.T., Böhlke, J.K., Bekins, B.A., Phillips, S.P., 2010. Mixing effects on apparent reaction rates and isotope fractionation during denitrification in a heterogeneous aquifer. Water Resour. Res. 46, W08525. doi:10.1029/2009WR008903, pp. 1–19.

Green, C.T., Puckett, L.J., Böhlke, J.K., Bekins, B.A., Phillips, S.P., Kauffman, L.J., Denver, J.M., Johnson, H.M., 2008. Limited occurrence of denitrification in four shallow aquifers in agricultural areas of the United States. J. Environ. Qual. 37 (3), 994–1009.

Haggerty, R., Schroth, M.H., Istok, J.D., 1998. Simplified method of 'push-pull' test data analysis for determining in situ reaction rate coefficients. Ground Water 36 (2), 314–324.

Hansen, D.E., Kume, J., 1970. Geology and Ground Water Resources of Grand Forks County: Part 1, Geology. North Dakota Geol. Survey Bull. 53, 76p.

Heron, G., Crouzet, C., Bourg, A.C.M., Christensen, T.H., 1994. Speciation of Fe(II) and Fe(III) in contaminated aquifer sediments using chemical extraction techniques. Environ. Sci. Technol. 28 (9), 1698–1705.

Kammer, A.E., 2001. Laboratory Denitrification Using Sediments from the Elk Valley Aquifer, Master's Thesis, Department of Geology and Geological Engineering, University of North Dakota, Grand Forks, North Dakota, 76p.

Kawanishi, T., Hayashi, Y., Kihou, N., Yoneyama, T., Ozaki, Y., 1993. Dispersion effect on the apparent nitrogen isotope fractionation factor associated with denitrification in soil: evaluation by a mathematical model. Soil Biol. Biochem. 25 (3), 349–354.

Kendall, C., 1998. Tracing nitrogen sources and cycling in catchments. In: Kendall, C., McDonnell, J.J. (Eds.), Isotope Tracers in Catchment Hydrology. Elsevier, Amsterdam, pp. 519–576.

Kennedy, L.G., Everett, J.W., Dewers, T., Pickins, W., Edwards, D., 1999. Application of mineral iron and sulfide analysis to evaluate natural attenuation at fuel contaminated site. J. Environ. Eng. 125 (1), 47–56.

Kölle, W., Strebel, O., Böttcher, J., 1985. Formation of sulfate by a microbial denitrification in a reducing aquifer. Water Supply 3 (1), 35–40.

Korom, S.F., 1991. Comment on "modeling of multicomponent transport with microbial transformation in groundwater: the Fuhrberg case" by E.O. Frind et al.. Water Resour. Res. 27 (12), 3271–3274.

Korom, S.F., 1992. Natural denitrification in the saturated zone: a review. Water Resour. Res. 28 (6), 1657–1668.

Korom, S.F., Schlag, A.J., Schuh, W.M., Schlag, A.K., 2005. In situ mesocosms: denitrification in the Elk Valley aquifer. Ground Water Monit. Remediat. 25 (1), 79–89.

Lawrence, A.R., Foster, S.S.D., 1986. Denitrification in a limestone aquifer in relation to the security of low-nitrate water supplies. J. Inst. Water Eng. Sci. 40 (2), 159–172.

Moncaster, S.J., Bottrell, S.H., Tellam, J.H., Lloyd, J.W., Konhauser, K.O., 2000. Migration and attenuation of agrochemical pollutants: insights from isotopic analysis of groundwater sulphate. J. Contam. Hydrol. 43, 147–163.

Mariotti, A., Germon, J.C., Leclerc, A., 1982. Nitrogen isotope fractionation associated with the $NO_2 \rightarrow N_2O$ step of denitrification in soils. Can. J. Soil Sci. 62 (2), 227–241.

Mariotti, A., Landreau, A., Simon, B., 1988. ^{15}N isotope biogeochemistry and natural denitrification process in groundwater: application to the chalk aquifer of northern France. Geochim. Cosmochim. Acta 52 (7), 1869–1878.

McKenzie, R.A., Rayner, A.C., Thompson, G.K., Pidgeon, G.F., Burren, B.R., 2004. Nitrate–nitrite toxicity in cattle and sheep grazing Dactyloctenium radulans (button grass) in stockyards. Aust. Vet. J. 82 (10), 630–634.

McMahon, P.B., Böhlke, J.K., Bruce, B.W., 1999. Denitrification in marine shales in northeastern Colorado. Water Resour. Res. 35 (5), 1629–1642.

Mengis, M., Walther, U., Bernasconi, S.M., Wehrli, B., 2001. Limitations of using $\delta^{18}O$ for the source identification of nitrate in agricultural soils. Environ. Sci. Technol. 35 (9), 1840–1844.

Mohamed, M.A.A., Terao, H., Suzuki, R., Babiker, I.S., Ohta, K., Kaori, K., Kato, K., 2003. Natural denitrification in the Kakamigahara groundwater basin, Gifu prefecture, central Japan. Sci. Total Environ. 307 (1–3), 191–201.

Parkhurst, D.L., Appelo, C.A.J., 1999. Users Guide to PHREEQC (Version 2): A Computer Program for Speciation, Batch-reaction, One-dimensional Transport, and Inverse Geochemical Calculations. US Geological Survey Water Resources Investigations Report 99-4259, 312 p.

Pauwels, H., Kloppmann, W., Foucher, J., Martelat, A., Fritsche, V., 1998. Field tracer test for denitrification in a pyrite-bearing schist aquifer. Appl. Geochem. 13 (6), 767–778.

Pauwels, H., Foucher, J., Kloppmann, W., 2000. Denitrification and mixing in a schist aquifer: influence on water chemistry and isotopes. Chem. Geol. 168, 307–324.

Phipps, G.C., Betcher, R.N., 2003. The Source and Fate of Groundwater Nitrate Beneath a Field Fertilized with Hog Manure: Assiniboine Delta aquifer, Manitoba, Canada. 4th Joint IAN-CNC/CGS Conference, Winnipeg.

Pickens, J.F., Cherry, J.A., Grisak, G.E., Merritt, W.F., Risto, B.A., 1978. A multilevel device for ground-water sampling and peizometric monitoring. Ground Water 16 (5), 322–327.

Postma, D., 1990. Kinetics of nitrate reduction by detrital Fe(II)–silicates. Geochim. Cosmochim. Acta 54 (3), 903–908.

Postma, D., Boesen, C., Kristiansen, H., Larsen, F., 1991. Nitrate reduction in an unconfined sandy aquifer: water chemistry, reduction processes, and geochemical modeling. Water Resour. Res. 27 (8), 2027–2045.

Schlag, A.J., 1999. In-situ Measurement of Denitrification in the Elk Valley Aquifer, Master's Thesis, Department of Geology and Geological Engineering, University of North Dakota, Grand Forks, North Dakota, 104p.

Schuh, W.M., Bottrell, S.H., Korom, S.F., Gallagher, J.R., Patch, J.C., 2006. Sources and Processes Affecting the Distribution of Dissolved Sulfate in the Elk Valley Aquifer in Grand Forks County, Eastern North Dakota. North Dakota State Water Commission Water Resources Investigation No. 38, 132p <http://www.swc.state.nd.us/4dlink9/4dcgi/GetContentRecord/PB-703>.

Schuh, W.M., Hove, M., Wanek, A., 2002. Initial assessment of nitrate-N load, load densities and loading rates in the Karlsruhe aquifer, ND, 2001. In: Preliminary Analysis of Nitrate-N Loads, and Causes of Nitrate-N Loading in the Karlsruhe and New Rockford Aquifers Near Karlsruhe, North Dakota in 2001. Report to the North Dakota Department of Health, February, 2002. North Dakota State Water Commission, Bismarck, ND.

Schultz, L.G., Tourtelot, H.A., Gill, J.R., Boerngen, J.G., 1980. Composition and Properties of the Pierre Shale and Equivalent Rocks, Northern Great Plains region. US Geological Survey Professional Paper 1064-B, 114p.

Spalding, R.F., Exner, M.E., 1993. Occurrence of nitrate in groundwater – a review. J. Environ. Qual. 22 (3), 392–402.

Spencer, E.J., 2003. Isotopic Tracers as Evidence of Denitrification in the Karlsruhe Aquifer, Master's Thesis, Department of Geology and Geological Engineering, University of North Dakota, Grand Forks, North Dakota, 58p.

Starr, R.C., Gillham, R.W., 1989. Controls on denitrification in shallow unconfined aquifers. Contaminant transport in groundwater. In: Proc. symposium, Stuttgart, 1989, pp. 51–56.

Stenger, R., Barkle, G., Burgess, C., Wall, A., Clague, J., 2008. Low nitrate contamination of shallow groundwater in spite of intensive dairying: the effect of reducing conditions in the vadose zone-aquifer continuum. J. Hydrol. NZ 47 (1), 1–24.

Tarits, C., Aquilina, L., Ayraud, V., Pauwels, H., Davy, P., Touchard, F., Bour, O., 2006. Oxido-reduction sequence related to flux variations of groundwater from a fractured basement aquifer (Ploemeur area, France). Appl. Geochem. 21, 29–47.

Tesfay, T., 2006. Modeling Groundwater Denitrification by Ferrous Iron Using PHREEQC, Doctoral Dissertation, Department of Geology and Geological Engineering, University of North Dakota, Grand Forks, North Dakota, 162p.

Tesoriero, A.J., Liebscher, H., Cox, S.E., 2000. Mechanism and rate of denitrification in an agricultural watershed: electron and mass balance along groundwater flow paths. Water Resour. Res. 36 (6), 1545–1559.

Tourtalot, H.S., 1962. Preliminary Investigation of the Geologic Setting and Chemical Composition of the Pierre Shale, Great Plains region. US Geological Survey Professional Paper 390, 74 p.

Warne, J.M., 2004. Design and Evaluation of a Modified In Situ Mesocosm to Study Denitrification in the Karlsruhe Aquifer, Master's Thesis, Department of Geology and Geological Engineering, University of North Dakota, Grand Forks, North Dakota, 62p.